Inflammation, Vol. 46, No. 4, August 2023 (© 2023)
https://doi.org/10.1007/s10753-023-01824-3

RESEARCH

Bacterial and Metabolic Factors of Staphylococcal Planktonic and Biofilm Environments Differentially Regulate Macrophage Immune Activation

Elisabeth Seebach[1,4] , Tabea Elschner[1,3] , Franziska V. Kraus[2] , Margarida Souto-Carneiro[2] and Katharina F. Kubatzky[1,4]

Received 15 February 2023; accepted 17 April 2023

Abstract— Biofilm formation is a leading cause for chronic implant-related bone infections as biofilms shield bacteria against the immune system and antibiotics. Additionally, biofilms generate a metabolic microenvironment that shifts the immune response towards tolerance. Here, we compared the impact of the metabolite profile of bacterial environments on macrophage immune activation using *Staphylococcus aureus* (SA) and *epidermidis* (SE) conditioned media (CM) of planktonic and biofilm cultures. The biofilm environment had reduced glucose and increased lactate concentrations. Moreover, the expression of typical immune activation markers on macrophages was reduced in the biofilm environment compared to the respective planktonic CM. However, all CM caused a predominantly pro-inflammatory macrophage cytokine response with a comparable induction of *Tnfa* expression. In biofilm CM, this was accompanied by higher levels of anti-inflammatory *Il10*. Planktonic CM, on the other hand, induced an IRF7 mediated *Ifnb* gene expression which was absent in the biofilm environments. For SA but not for SE planktonic CM, this was accompanied by IRF3 activation. Stimulation of macrophages with TLR-2/-9 ligands under varying metabolic conditions revealed that, like in the biofilm setting, low glucose concentration reduced the *Tnfa* to *Il10* mRNA ratio. However, the addition of extracellular L-lactate but not D-lactate increased the *Tnfa* to *Il10* mRNA ratio upon TLR-2/-9 stimulation. In summary, our data indicate that the mechanisms behind the activation of macrophages differ between planktonic and biofilm environments. These differences are independent of the metabolite profiles, suggesting that the production of different bacterial factors is ultimately more important than the concentrations of glucose and lactate in the environment.

KEY WORDS: Implant-related bone infections; Staphylococcus; Biofilm; Macrophages; Immune response; Metabolites.

[1]Department of Infectious Diseases, Medical Microbiology and Hygiene, Heidelberg University, Im Neuenheimer Feld 324, 69120 Heidelberg, Germany
[2]Department of Internal Medicine 5 - Hematology Oncology Rheumatology, Heidelberg University Hospital, Im Neuenheimer Feld 410, 69120 Heidelberg, Germany
[3]Current address: Institute for Cardiovascular Sciences & Institute of Neurovascular Cell Biology (INVZ), University Hospital Bonn, University of Bonn, Bonn, Germany
[4]To whom correspondence should be addressed at and Department of Infectious Diseases, Medical Microbiology and Hygiene, Heidelberg University, Im Neuenheimer Feld 324, 69120, Heidelberg, Germany. Email: elisabeth.seebach@med.uni-heidelberg.de kubatzky@uni-heidelberg.de

INTRODUCTION

Chronic implant-related bone infections are a major complication in orthopedic and trauma surgery with severe consequences for the patients including long-term antibiotic treatment, repeated surgeries, implant revision, and at worst amputation of the infected limb [1, 2]. Bacteria can take advantage of the indwelled, foreign body and form biofilms on the implant surface. Such infections are frequently persistent because the biofilm matrix acts as a physical barrier that shields bacteria against eradication through the host immune system and antibiotic treatment [3–6]. Furthermore, several studies show that biofilm formation promotes a more tolerant immune response, which facilitates bacterial persistence [7, 8].

Staphylococcus aureus (SA) and *epidermidis* (SE) are the most frequently isolated bacteria in implant-related bone infections [1, 6]. SA expresses a broad range of virulence factors, is able to form small colony variants (SCV), can survive inside osteoblasts and osteoclasts [9, 10], persists in cortical bone structures [11], and forms biofilms [12]. The commensal SE in comparison mainly relies on biofilm formation as an immune evasion strategy but does not produce aggressive pathogenic factors [13, 14]. Thus, SA is predominantly found in early and acute infections that are associated with pain, swelling, and fever and implicate a high risk for infection recurrence after antibiotic and surgical treatment [15]. SE causes only mild symptoms and low-grade inflammation. Therefore, SE infections are commonly detected when the infection gets chronic, which is closely linked to biofilm formation [16].

Recognition of specific bacterial pathogen-associated molecular patterns (PAMPs) by innate immune cells causes activation of pattern recognition receptors (PRRs), such as the toll-like receptors (TLRs). Binding of a PAMP to its respective TLR leads to the activation of the nuclear factor "kappa-light-chain-enhancer" of activated B cells (NF-κB) pathway and subsequent to the induction of inflammatory cytokines. Furthermore, TLR activation can induce a Type 1 IFN response mainly via the IRF7 pathway resulting in the production of IFN-α and IFN-β [17]. Next to TLRs, cytosolic PRRs including Nod-like receptors (NLRs) and dsDNA sensors such as cGAS/STING contribute to an effective immune response against invading bacteria [18, 19]. Binding of SA lipopeptides and lipoteichoic acid (LTA) triggers immune cell activation through surface-bound TLR-2 while the recognition of bacterial DNA motifs occurs via endosomal TLR-9 [20]. Biofilm formation, however, is discussed to prevent TLR-2 and TLR-9 recognition of embedded bacteria by masking or retaining PAMPs within the biofilm matrix [21, 22].

Macrophages are innate immune cells with an important role in the first line of defense against invading pathogens. Together with the other cells of the innate immune system, they fight bacterial infections by phagocytosis and production of anti-microbial molecules such as nitric oxygen (NO), anti-microbial peptides, and cytokines [23]. *In vitro*, macrophages can be polarized into rather pro-inflammatory (M1) or anti-inflammatory (M2) phenotypes [24], associated either with bacterial clearance or tolerance and persistence, respectively [25]. This classification is defined by the presence of specific surface markers, expression of inducible nitric oxide synthase (iNOS, M1) or arginase 1 (Arg-1, M2), and the cytokine profile of the respective macrophage population (M1: TNF-α, IL-1, and IL-12 vs. M2: IL-10 and TGF-β) [25]. Macrophage subtypes are also characterized by different metabolic activities. While M1 macrophages predominantly rely on aerobic glycolysis, M2 macrophages are associated with oxidative phosphorylation (OxPhos) [26]. Usually, an effective pro-inflammatory macrophage immune response is able to clear an infection caused by planktonic bacteria. However, this often fails once these bacteria start building a biofilm. Metabolically, biofilm formation is characterized by the extraction of glucose from the environment and the accumulation of fermentation products such as lactate due to the anaerobic growth conditions within the biofilm [27]. This metabolic microenvironment is considered to support the biofilm-mediated anti-inflammatory macrophage polarization and thus impairs them to exert their clearance functions [28].

So far, most studies focused on the investigation of the infection after a biofilm has formed. Our aim was to compare the macrophage immune response between the planktonic and biofilm scenario and to evaluate potential differences regarding a pro- or anti-inflammatory macrophage polarization. Special focus was set on the question whether different metabolite levels could be central for the distinct macrophage activation by planktonic and biofilm environments, or if this was rather triggered by the varying presence of bacterial factors. To address this question, we treated murine RAW 264.7 macrophages with conditioned media (CM) generated from SA or SE planktonic and biofilm cultures, respectively, and analyzed the induction of a pro- or anti-inflammatory macrophage response and the metabolic activity. Additionally, we

evaluated the effect of low glucose or high lactate concentrations on macrophage polarization upon combined TLR-2/-9 stimulation or treatment with SA planktonic CM.

MATERIALS AND METHODS

Bacteria Culture and Preparation of Conditioned Media

Staphylococcus aureus strain ATCC 49230 (UAMS-1, isolated from a patient with chronic osteomyelitis) [29] and *Staphylococcus epidermidis* strain DSM 28319 (RP62A, isolated from a catheter sepsis) were used for the preparation of conditioned media. Bacteria were cultured on Columbia agar plates with 5% sheep blood (BD, Germany) and streaked onto fresh agar plates a day before experiment. Three to 5 colonies were transferred into trypticase soy bouillon (TSB; BD, Germany) and cultivated under shaking for 3 h at 37 °C to receive growth state bacteria. Bacterial density was measured photometrically (Den-1, Grant Instruments, UK) and adjusted to a concentration of $6*10^5$ CFU/ml in DMEM high glucose (Anprotec, Germany) + 10% heat-inactivated fetal calf serum (FCS; Biochrom GmbH, Germany). For planktonic culture, bacteria were cultivated under shaking (200 rpm) for 24 h at 37 °C and 5% CO_2. For biofilm culture, bacteria were plated in 24 well with 1 ml per well and cultivated under static conditions for 6 days. In biofilm cultures, medium was carefully replaced every 24 h. For CM, planktonic medium after 24 h of culture or the last 24 h medium change before day 6 biofilm culture was harvested by centrifugation at 4000 rpm for 15 min at 4 °C. For biofilm CM, the media of wells were pooled before centrifugation. Harvested media were streaked onto agar plates and cultivated overnight at 37 °C, and bacterial appearance (colony size and color) was controlled to ensure no contamination by other bacteria. Supernatants were then sterile filtered through a 0.2 µm filter and frozen at − 80 °C. To rule out remaining bacterial growth, sterile filtered media were inoculated in TSB and cultivated overnight at 37 °C. Before use in cell culture, pH of CM was adjusted to physiological pH of growth medium (DMEM high glucose + 10% FCS) by drop-by-drop titration with 0.5 N NaOH and color check of the pH indicator Phenol Red. Aliquots were stored at − 80 °C. Planktonic and biofilm CM from the same approach were compared within one experiment. For unstimulated CM control, growth medium (DMEM high glucose + 10% FCS) of the respective approach was treated analogously to CM without bacteria inoculation.

^{1}H NMR Metabolomics

^{1}H NMR spectra of one representative CM approach were acquired using a 400 MHz Bruker spectrometer (Bruker Ultrashield™ Plus 400) equipped with a 5-mm indirect detection probe. Each spectrum covered a spectral width of 6.4 kHz. A NOESY1D sequence with water-signal suppression and a 30° pulse and a total repetition time of 6.5 s were applied to ensure full relaxation of all proton nuclei in the samples. Before Fourier transformation, each free induction decay (FID) was multiplied by a decaying exponential with a decay constant of 0.3 Hz. To allow comparison between different spectra, sodium fumarate (10 mM), dissolved in a 0.2 M phosphate buffer solution prepared with D_2O (99.9%), was used as an internal standard. NMR samples consisted of 140 µl of CM plus 35 µl of fumarate standard. Before evaluation, spectra were phase adjusted and baseline corrected using the Bruker TopSpin 3.6.3 software. Spectra were further calibrated by setting the resonance of fumarate to $\delta = 6.5$ parts per million (ppm). For comparison of different CM, spectra were adjusted to each other by equalizing the resonance of fumarate.

Cell Culture and Stimulation of Macrophages

The murine macrophage cell line RAW 264.7 (ATCC TIB-71, USA) was used for the experiments [30]. RAW 264.7 cells were cultivated in DMEM high glucose + 10% heat-inactivated FCS + 1% Pen/Strep at 37 °C and 5% CO_2. Cells were plated into suitable well plate formats, treated with CM 1:1 diluted in fresh cell growth media or PC (positive control: 1 µg/ml TLR-2 ligand Pam3CSK4 and 100 nM TLR-9 ligand CpG ODN 1668, both InvivoGen, USA). For experiments with different glucose concentrations, cells were cultivated one passage before experiment either in high glucose DMEM (4.5 g/l) or low glucose DMEM (1 g/l, Anprotec, Germany) and following stimulation was done in medium with the respective glucose concentration. In experiments with different extracellular lactate concentrations, sodium L- or D-lactate (10, 15, and 20 mM, both Sigma-Aldrich, Germany) were added simultaneously to stimulation.

Flow Cytometry

For FACS analysis, 2 million cells/well were plated with 1 ml fresh growth media and 1 ml CM. After 20 h, supernatants were frozen at − 80 °C for further investigation, and cells were washed twice with cold PBS. For

surface marker staining, 100 µl of cell suspension was either left in PBS/2% BSA for the unstained control or stained with 0.2 mg/ml FITC anti-TLR-2 (Novus Biologicals, UK), PE anti-MHC II (Invitrogen, USA), PE anti-CD80 or PE anti-CD86 (both BioLegend, USA) antibodies at 4 °C for 1 h. Cells were washed two times in cold PBS, resuspended in 150 µl cold PBS, and then analyzed with the BD FACSCanto™ Flow Cytometer (BD Biosciences, USA). After measurement, unstained controls were additionally incubated with 30 nM SYTOX™ Green nucleic acid stain (Invitrogen, USA) for 5 min, and live/dead contribution was recorded. For intracellular staining of TLR-9, 500 µl of cell suspension were combined with 500 µl fixation buffer (BioLegend, USA), incubated at 37 °C for 15 min, centrifuged at 2000 rpm for 5 min, washed twice with PBS/5% BSA, and then stored at 4 °C, overnight in PBS/5% BSA. The next day, cells were centrifuged and resuspended in 1 ml of − 20 °C cold TruePhos™ Perm Buffer (BioLegend, USA) and incubated at − 20 °C for 1 h. Cells were then washed two times and resuspended in 500 µl PBS/2% BSA. A total of 100 µl of cell suspension was either kept unstained, stained with 0.5 mg/ml Alexa647 anti-TLR-9 antibody (Novus Biologicals, UK) or respective isotype at RT for 30 min. Cells were washed twice, resuspended in 300 µl PBS/2% BSA and analyzed with the BD FACSCanto™ Flow Cytometer. Results were further analyzed using the Flowing Software (version 2.5.1, Turku Bioscience, Finland).

Cytometric Bead Array

Supernatants of FACS surface marker analysis were used for cytometric bead array (CBA, LEGENDplex™, BioLegend, USA) according to the manufacturer's protocol. A Mouse Inflammation Panel (Mix and Match Subpanel) was used including beads against TNF-α, IL-10, and IFN-β. In short, supernatants were centrifuged and diluted 1:5 with Assay Buffer; standard samples were prepared, and samples were transferred into a V-bottom plate. Bead mix was prepared, added to the samples, and incubated on a shaker overnight at 4 °C in the dark. The next day, plate was washed 2 times and incubated with detection antibody for 1 at RT while shaking. Streptavidin-phycoerythrin (SA-PE) was added and further incubated for 30 min at RT while shaking. Plate was washed two times; bead pellet was resuspended in wash buffer, and data acquisition was done with the BD® LSR II Flow Cytometer. Analysis and calculation of cytokine concentrations were performed with the included LEGENDplex™ Data Analysis Software (version 8.0).

Gene Expression Analysis

For gene expression analysis, cells were stimulated as indicated in the figure legends. Total RNA extraction was performed using the innuPREP RNA Mini Kit 2.0 (Analytik Jena, Germany) according to the manufacturer's protocol. In short, cells were scraped in lysis buffer and transferred to a DNA elimination column. RNA in the lysate was precipitated by adding 70% ethanol, transferred to an RNA column, washed, and eluated in H_2O. Total RNA concentration was measured using the NanoDrop® ND-1000 spectrophotometer (Thermo Scientific, Germany). One microgram of total RNA was subjected to cDNA synthesis using the Biozym cDNA synthesis Kit (Biozym Scientific GmbH, Germany) according to the manufacturer's protocol using Oligo (dT) primer. A noRT sample (w/o Reverse Transcriptase) consisting of pooled total RNA of all samples of one experiment was prepared. cDNA was diluted 1:1 in H_2O and stored at − 20 °C. Two microliters of cDNA template and 400 nM of respective primer pairs (Table 1) were used in qPCR. mRNA levels were evaluated in a two-step PCR reaction (StepOnePlus Real-Time PCR Cycler, Applied Biosystems, USA) with 60 °C annealing/extension temperature for 40 cycles using the 2 × qPCRBIO SyGreen Mix Hi-ROX (PCR Biosystems Ltd., UK). The quality of qPCR runs and specificity of qPCR products were controlled by included noRT and water samples for each experiment and primer pair and melting curve comparison. mRNA levels of the respective genes of interest (Table 1) were normalized to the reference gene *Hprt1* and calculated by the $2^{-\Delta CT}$ method.

Immunoblotting

For protein analysis by western blot, cells were stimulated as indicated in the figure legends. Cells were lysed in RIPA buffer (1% v/v NP-40 (IGEPAL® CA-630), 0.25% sodium deoxycholate, 50 mM Tris pH 8.0, 150 mM NaCl, 1 mM EDTA pH 8.0, 1 mM Na_3VO_4) with EDTA-free protease inhibitors (cOmplete™ Tablets) and phosphatase inhibitors (PhosSTOP™, both Roche Diagnostics GmbH, Germany) for 1 h at 4 °C under rotation. Lysates were centrifuged at 14,000 rpm for 20 min at 4 °C. Protein concentrations were determined by BCA assay (Cyanagen Srl, Italy), and samples were adjusted to 10 µg protein per 20 µl with ddH_2O and 5 µl 4 × SDS sample buffer with 10% β-mercaptoethanol and loaded on pre-cast gradient 4–20% Tris–glycine gels (anamed Elektrophorese GmbH, Germany). Proteins were transferred

Table 1 List of Oligonucleotides Used for Quantitative RT-PCR Analysis

Gene for	RefSeq	Forward primer	Reverse primer
Acod1	NM_008392.1	CAGCTCTATCGGAAGCCCTG	CAGAAACTTGGACGCAGCAG
Arg1	NM_007482.3	TCACCTGAGCTTTGATGTCG	CACCTCCTCTGCTGTCTTCC
Slc2a1	NM_011400.3	CAGTTCGGCTATAACACTGGTG	GCCCCCGACAGAGAAGATG
Hprt1	NM_013556.2	GGGGACATAAAAGTTATTGGTGG	CATTTTGGGGCTGTACTGCT
Ifnb	NM_010510.1	TGGGAGATGTCCTCAACTGC	CCAGGCGTAGCTGTTGTACT
Il6	NM_031168.2	CCGGAGAGGAGACTTCACAG	TTCTGCAAGTGCATCATCGT
Il10	NM_010548.2	GGTTGCCAAGCCTTATCGGA	ACCTGCTCCACTGCCTTGCT
Isg15	NM_015783.3	CCTGGTGAGGAACGAAAGGG	AAGCGTGTCTACAGTCTGCG
Nos2	NM_010927.4	CATGAGCTTGGTGTTTGGGTG	TCCGCAAATGTAGAGGTGGC
Tnfa	NM_013693.3	AAAATTCGAGTGACAAGCCTGTAG	CCCTTGAAGAGAACCTGGGAG TAG

Mouse-specific primers were designed intron-flanking and included all transcript variants if possible and were obtained from biomers.net GmbH, Germany. If more transcript variants are present, RefSeq is given for transcript variant 1

onto an Amersham™ Protran™ 0.45 µm nitrocellulose membrane (GE Healthcare, UK). Membranes were blocked with BlueBlock PF (Serva Electrophoresis GmbH, Germany) for 30 min at RT before incubation with primary antibodies (Table 2) overnight at 4 °C. After three times washing with TBST, membranes were incubated with an anti-rabbit HRP-linked secondary antibody (1:1000, Cell Signaling Technology, USA) for 1 h at RT. Blots were developed with ECL substrate (WESTAR ETA C ULTRA 2.0, Cyanagen Srl, Italy) and imaged in the ChemoStar ECL & Fluorescence Imager (Intas Science Imaging Instruments GmbH, Germany).

L-Lactate Detection

A total of 50,000 cells/well were plated in 96-well format and stimulated with 100 µl CM and 100 µl fresh growth media for 24 h. Supernatants of three replicates were pooled and stored at − 80 °C until further processing. L-lactate concentration was measured in CM as well as in supernatants of CM stimulated macrophages using an enzyme-based bioluminescent assay according to the manufacturer's protocol (Lactate-Glo™ Assay, Promega GmbH, Germany). CM and supernatants were used 1:50 (planktonic CM) or 1:100 (other) diluted with PBS, a standard curve with defined L-lactate concentrations (0–200 µM) was included. Samples and standard were incubated with the lactate detection reagent for 1 h at RT, and light emission was recorded by luminometer (LUMIstar® Optima, BMG LABTECH, Germany).

ATP Detection

A total of 50,000 cells/well were plated in 96-well format and stimulated with 100 µl CM and 100 µl fresh growth media for 24 h. Samples were performed in triplicates. Media were removed, and 100 µl of CTG reagent (CellTiter-Glo®, Promega GmbH, Germany; 1:1 with PBS) per well was added. Cells were lysed for 1 min at RT

Table 2 List of Antibodies Used for Immunoblotting (Western Blot)

Protein	Source	Size (kDa)	Dilution	Company
HSP-90	Rabbit	90	1:1000	Cell Signaling Technology, USA
Phospho-IRF3 (Ser396)	Rabbit	45–55	1:1000	Cell Signaling Technology, USA
Phospho-IRF7 (Ser437/438)	Rabbit	55	1:1000	Cell Signaling Technology, USA
Phospho-NFκB p65 (Ser536)	Rabbit	65	1:1000	Cell Signaling Technology, USA

Antibodies were all recommended for use in mouse and applied according to the manufacturer's advice. Proteins were detected by chemiluminescent luminol reaction after incubation with respective HRP-linked secondary antibody and imaged in a ChemoStar ECL Imager

under continuous shaking. After 10 min incubation in the dark, supernatants were transferred into a white 96-well plate. Relative ATP content was determined by bioluminescent light reaction in a luminometer (LUMIstar® Optima, BMG LABTECH, Germany).

Mitochondrial Activity

A total of 300,000 cells/well were transferred in 24 well plates and stimulated with CM 1:1 diluted with fresh growth media in a total of 1 ml. Mitochondrial activity was measured after 24 h by adding 100 nM of a mitochondrial membrane potential-sensitive dye (stock conc.: 1 mM in DMSO, MitoTracker® Deep Red FM, Cell Signaling Technology, USA) to the cells for 30 min at 37 °C and 5% CO_2. Cells were then washed three times with cold PBS, scraped in PBS, and transferred into FACS tubes. Mitochondrial activity was analyzed with the BD FACSCanto™ Flow Cytometer according to the fluorescence intensity of the dye. Only the living cell population was included in further analysis using the Flowing Software (version 2.5.1, Turku Bioscience, Finland).

Statistical Analysis

Experiments were done in $n = 4$ or 5 independent replicates as stated in the figure legends. Data are presented as mean + SD and single values as dots. Statistical evaluation was performed using ordinary one-way ANOVA with post hoc multiple comparison testing and the Bonferroni correction. A p-value below 0.05 was considered statistically significant. Asterisk is indicating significance against Medium, and number sign is showing significance between different treatments. Data analysis was performed with GraphPad Prism for Windows (Version 9.3.1, GraphPad Software Inc., USA).

RESULTS

In Vitro Generated CM Represent the *In Vivo* Biofilm Environment Characterized by Low Glucose and High Lactate Levels

To validate the experimental system, we monitored the ability of the two bacterial strains, SA and SE, to form biofilms. As described in the literature, we could reproduce that SA strain UAMS-1 is a moderate biofilm producer on non-coated plastic surfaces *in vitro* [31], whereas SE RP62A is known to possess strong *in vitro* biofilm formation capacities on plastic [32] (Fig. 1A, B). Supernatants were prepared from bacterial cultures under planktonic or biofilm-specific culture conditions (Fig. 1B, C). ^{1}H-NMR analysis of these supernatants revealed that glucose could still be detected in the CM of planktonic SA and SE, whereas all glucose was metabolized in the respective biofilm CM (Fig. 1D). In all conditions, bacteria released acetate. Interestingly, the levels differed between SA and SE and were higher in CM from planktonic SA and biofilm SE. As lactate was strongly increased in the CM of SA and SE biofilm cultures, but could only be detected in residual amounts in the respective planktonic CM, we conclude that the generated CM represent the *in vivo* situation, characterized by glucose deprivation and lactate accumulation.

All CM Induce a Pro-Inflammatory Macrophage Immune Response, Which Is Less Pronounced in Biofilm CM

To evaluate potential differences in the activation of macrophages by either the planktonic or biofilm environments of SA and SE, we stimulated RAW 264.7 macrophages with the respective CM. As a control, we also stimulated cells with the TLR-2/-9 ligands Pam3CSK4 and CpG ODN (PC). Figure 2A shows that stimulation of macrophages with planktonic CM increased the surface protein expression of the immune activation markers TLR-2, MHC II, CD80 and CD86 much stronger than the respective biofilm CM. This is in line with previous findings that the biofilm environment promotes immune cell tolerance. Protein levels of intracellular TLR-9, however, were only slightly increased with no major differences between planktonic and biofilm CM. We further wanted to evaluate macrophage polarization. Therefore, we validated the induction of genes associated with the pro-inflammatory M1 or anti-inflammatory M2 phenotype by using established controls (Suppl. Figure 1). LPS/IFN-γ stimulation as well as our PC led to an increase in *Nos2* (gene encoding for iNOS), *Tnfa*, and *Ifnb* mRNA levels, whereas *Arg1* gene expression was only up-regulated by IL-4/IL-10 treatment. This indicates that gene expression levels of these immune mediators were valid to determine a more pro- or anti-inflammatory macrophage immune response. As TNF-α is associated with a pro-inflammatory (M1) and IL-10 with an anti-inflammatory (M2) macrophage phenotype, the ratio of the respective mRNA levels was used as an indicator of macrophage polarization. Accordingly,

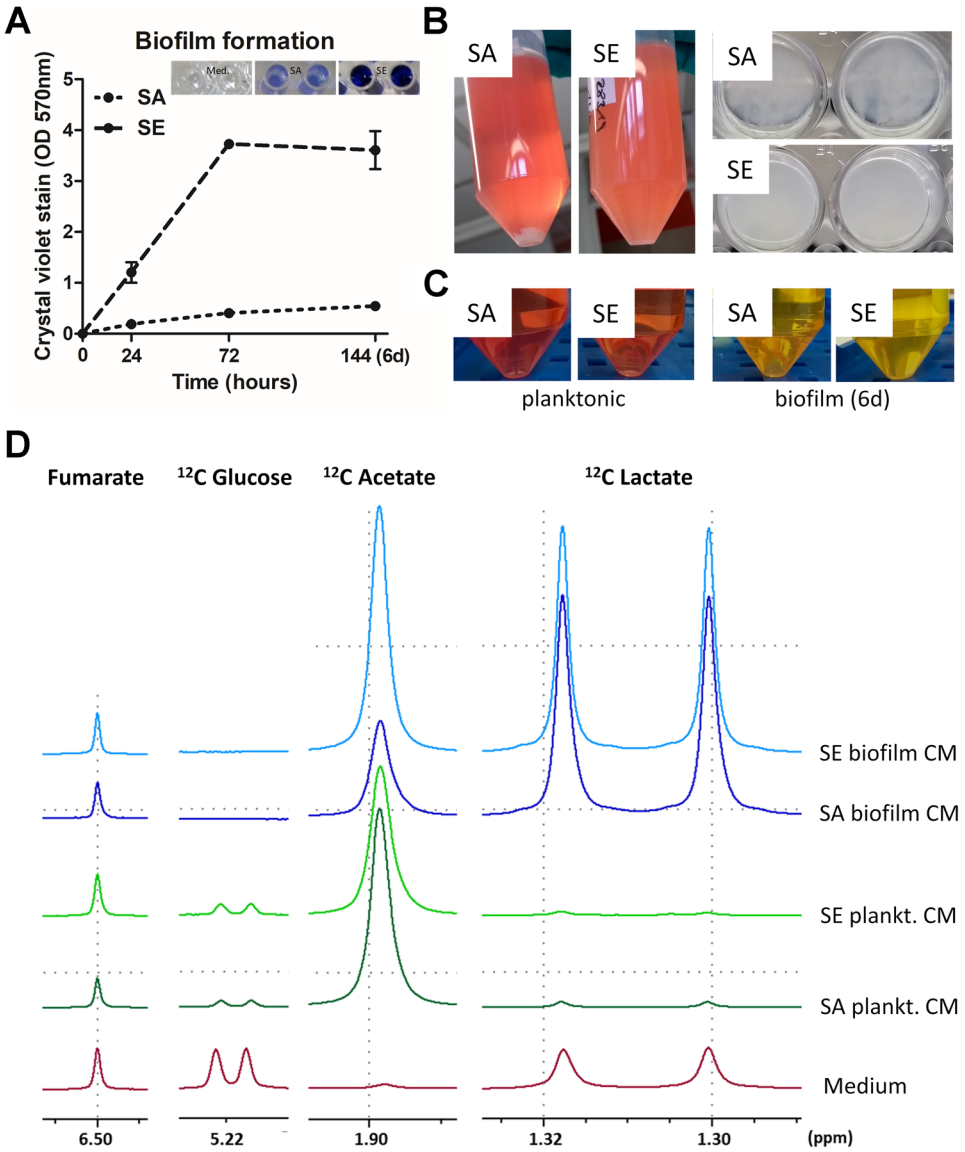

Fig. 1 Biofilm formation of selected bacteria strains and preparation and characterization of conditioned media. *Staphylococcus aureus* (SA) strain ATCC 49230 (UAMS-1) and *Staphylococcus epidermidis* (SE) strain DSM 28319 (RP62A) were used in this study. Bacteria were freshly streaked out a day before experiment. To generate log-phase bacteria, 3–5 colonies were transferred in TSB, cultured for 3 h, and then adjusted to 10^6 CFU per ml. **A** *In vitro* biofilm formation of study strains. A total of 100 µl of bacteria (10^5 CFU/ well) in TSB with 1% glucose were transferred into 96 well plates and cultivated at 37 °C for 24, 72, and 144 h. TSB with 1% glucose was replaced every 24 h. Biofilm formation was quantified by crystal violet staining (1% crystal violet in H_2O). Data are presented as OD at 570 nm which is proportional to biofilm mass. $n = 2$ experiments in triplicates, mean ± SD are shown. **B** Pictures showing planktonic cultures after 24 h of shaking and biofilm formation of static culture in 24 wells after 6 days. For generation of conditioned media (CM), bacteria ($6*10^5$ CFU/ well/ ml) were cultured in growth media (DMEM high glucose + 10% FCS) without antibiotics at 37 °C and 5% CO_2. During biofilm formation, media were replaced every 24 h. **C** Pictures of respective CM before pH adjustment. CM were harvested by centrifugation and sterile filtration after 24 h of planktonic culture or the last 24 h media of 6 days biofilm culture. **D** ^{1}H NMR spectra of CM were acquired using a 400 MHz Bruker spectrometer (Bruker Ultrashield™ Plus 400). To allow comparison between different spectra, sodium fumarate (10 mM), dissolved in a 0.2 M phosphate buffer solution prepared with D_2O (99.9%), was used as an internal standard. For comparison of different CM, spectra were adjusted to each other by equalizing the resonance of fumarate. Resonances of metabolites were then compared between the different CM. Shown are multiple display expansions of spectra of growth medium and CM for fumarate (singlet; $\delta = 6.50$ ppm), ^{12}C glucose (doublet; $\delta = 5.22$ ppm), ^{12}C acetate (singlet; $\delta = 1.90$ ppm), and ^{12}C lactate (doublet; $\delta = 1.31$ ppm).

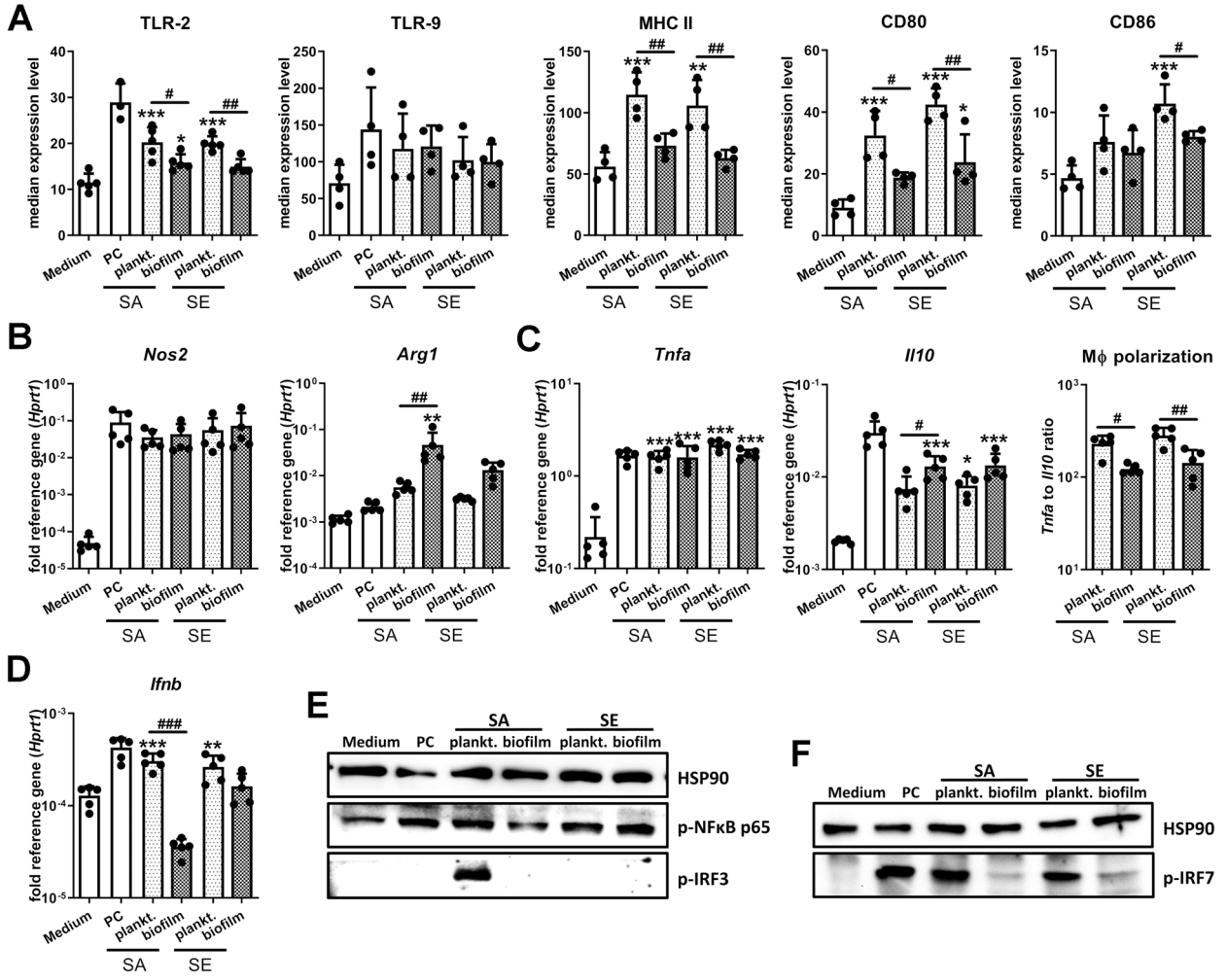

Fig. 2 Macrophage immune activation after stimulation with conditioned media. RAW 264.7 cells were cultivated in CM 1:1 diluted in fresh growth media (DMEM high glucose + 10% FCS + 1% Pen/Strep), and immune response was investigated. **A** Immune marker profile of macrophages. Cells were stimulated with CM for 20 h, and surface protein levels of TLR-2, MHC complex II (MHCII), co-stimulatory proteins CD80 and CD86 as well as endosomal TLR-9 were measured by FACS analysis. Data are presented as median expression levels measured by fluorescence intensity. $n = 4$ or 5 experiments. **B**–**D** Gene expression analysis of relevant immune mediators. Cells were stimulated with CM for 20 h, and mRNA levels of M1 marker *Nos2* and M2 marker *Arg1* (**B**), pro-inflammatory *Tnfa* and anti-inflammatory *Il10* (**C**), and *Ifnb* (**D**) were quantified by RT-qPCR. The ratio of *Tnfa* to *Il10* expression levels was used as an indicator for macrophage polarization. Data are presented as relative gene expression of gene of interest related to the reference gene *Hprt1*. $n = 5$ experiments. **E**, **F** Activation of NF-κB, IRF3, and IRF7 signaling in macrophages. Cells were stimulated with CM for 4 h, and the presence of phospho-NFκB p65 and phospho-IRF3 (**E**) or phospho-IRF7 (**F**) as activated forms of the transcription factors was visualized by western blot. HSP90 was used as loading control, $n = 3$ experiments. For **A**–**D**, data are presented as mean + SD, and single values are shown as dots. *p*-values are calculated by ordinary one-way ANOVA with post hoc Bonferroni-corrected multiple comparison. Asterisk indicates significance against Medium, and number sign shows significance between respective planktonic and biofilm CM. $*p < 0.05$, $**p < 0.01$, $***p < 0.001$; $\#p < 0.05$, $\#\#p < 0.01$, $\#\#\#p < 0.001$. PC, positive control (1 µg/ml Pam3CSK4 + 100 nM CpG ODN).

the *Tnfa*/*Il10* ratio was higher in the LPS/IFN-γ induced M1 macrophages (Suppl. Figure 1B). Unexpectedly, gene expression analysis of macrophages upon stimulation with CM revealed that *Nos2* was highly induced by both, planktonic as well as biofilm environments. However, mRNA levels of *Arg1* were only increased in biofilm CM (Fig. 2B). In line with this, all CM induced the expression of the pro-inflammatory cytokine *Tnfa* to a similar extent,

whereas mRNA levels of the anti-inflammatory cytokine *Il10* were higher in biofilm CM. The *Tnfa*/*Il10* ratio suggests an overall reduced pro-inflammatory macrophage polarization in biofilm compared to planktonic CM (Fig. 2C). Interestingly, in planktonic environments, we observed an induction of *Ifnb* gene expression, which was not detectable for the biofilm CM (Fig. 2D). The corresponding protein analysis corroborated that TNF-α secretion was increased for all CM treatments, with the lowest concentration found for SA planktonic CM. Also, IL-10 release was increased on the protein level after CM treatment, but in contrast to mRNA levels, no differences were observed between planktonic and biofilm environments (Suppl. Figure 2A). In line with the gene expression analysis, IFN-β protein levels were only increased after stimulation with planktonic CM (Suppl. Figure 2B). However, it has to be taken into account that high protein A contents in SA planktonic CM might have interfered with the antibody-based detection and contributed to the cytokine concentrations measured in the supernatants of samples treated with SA planktonic CM.

On the level of signal transduction, we found an activation of the NF-κB pathway as indicated by increased levels of phosphorylated p65 (Fig. 2E), which is in line with the observed increase in *Tnfa* and *Il10* expression. While SA and SE planktonic CM were able to trigger IRF7 phosphorylation, the master regulator of *Ifnb* induction, the IRF-3 pathway was only activated after treatment with SA planktonic CM. Also, the *Ifnb* gene expression caused by TLR activation was independent of phospho-IRF3 as only an activation of the IRF7 pathway was observed for PC (Figs. 2 E, F). To rule out that the observed differences between planktonic and biofilm CM were due to cell viability, we stained for dead cells, but could not detect any differences between the treatment groups (Suppl. Figure 2C). Thus, our data suggest that both planktonic as well as biofilm CM lead to a pro-inflammatory macrophage immune response; however, the expression of immune surface markers was less prominent after treatment with biofilm CM, and the induction of an IFN-β response was limited to planktonic CM.

Macrophage Immune Response Is Dominated by Glycolytic Metabolism with a Shift Towards Increased Mitochondrial Activity in SE Biofilm CM

As the metabolic state shapes the activity of immune cells and supports immune cell polarization, we analyzed the metabolic activity of RAW 264.7 macrophages upon CM treatment. In a first step, we investigated the levels of L-lactate in the CM. As expected from the ^{1}H-NMR results, only low levels of L-lactate were present in planktonic CM, whereas biofilm CM contained high amounts of bacteria- derived L-lactate (Fig. 3A). Next, we measured L-lactate levels from RAW macrophage cultures after stimulation with the CM. Here, we detected increased L-lactate concentrations in the supernatants of all culture conditions. However, it has to be considered that the L-lactate generated by the bacteria during biofilm formation contributed to the L-lactate concentrations present in the supernatant of macrophages treated with biofilm CM (Fig. 3B). Thus, we corrected the measured L-lactate concentrations in the macrophage supernatants with the theoretical L-lactate concentration delivered by the respective CM 1:1 diluted in fresh cell culture media. The calculated L-lactate production by the macrophages indicated an increased aerobic glycolysis of the cells especially in the planktonic environment (Fig. 3C). Aconitate decarboxylase 1 (ACOD-1, also known as IRG-1) catalyzes the reaction of cis-aconitate into the anti-inflammatory itaconate and thus interrupts the Krebs cycle, shifting cellular metabolic activity towards glycolysis [33, 34]. *Acod1* gene expression was induced upon stimulation with the CM (Fig. 3D). A mitochondrial activity assay revealed that also mitochondrial activity was induced after stimulation with the CM. This was most pronounced in the biofilm environment of SE biofilm (Fig. 3E). Total ATP levels remained similar across all treatment conditions (Fig. 3F).

Overall, our data corroborate that in a pro-inflammatory scenario macrophage metabolism mainly relies on aerobic glycolysis. Again, this was found to be more pronounced in the planktonic environment. Especially for SE, a shift towards increased mitochondrial activity become apparent in the biofilm environment, which generally is associated with an anti-inflammatory polarization of the immune response.

Low Glucose and High Lactate Levels Only Show Moderate but Slightly Different Effects on Macrophage Cytokine Response upon TLR-2/-9 Stimulation

To investigate if the changes in the macrophage activity pattern were primarily caused by the observed shift in metabolite abundance in the biofilm environment, we stimulated RAW 264.7 macrophages with the TLR ligands Pam3CSK4 and CpG ODN (PC) in the presence of high (4.5 g/l) and low (1 g/l) glucose levels or different

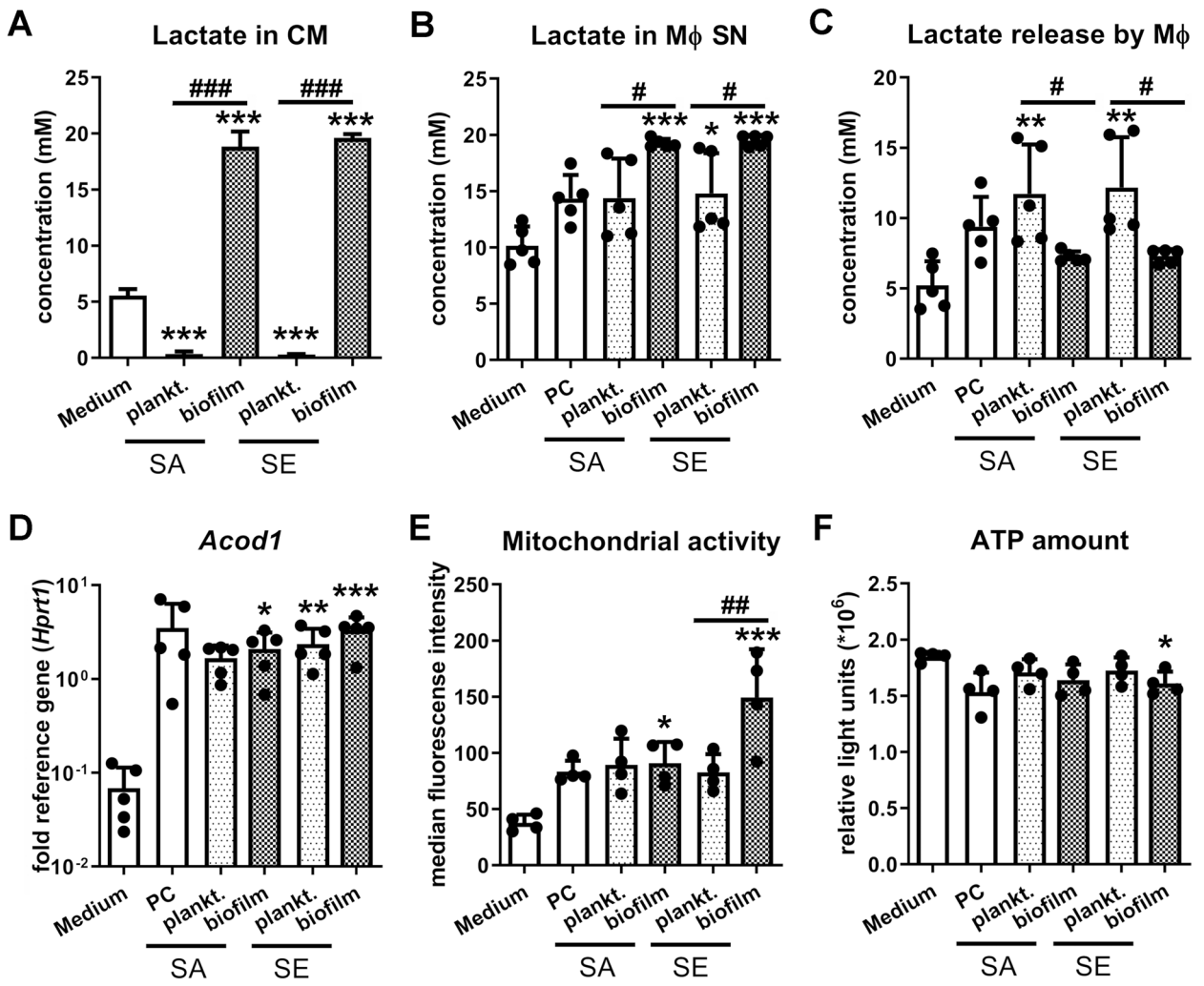

Fig. 3 Metabolic changes in macrophages after stimulation with conditioned media. RAW 264.7 cells were cultivated in CM 1:1 diluted in fresh growth media (DMEM high glucose + 10% FCS + 1% Pen/Strep), and metabolic parameters were investigated. **A** L-lactate amount in conditioned media. Bacteria were cultivated either in planktonic culture for 24 h or biofilm culture for 6 days. CM were harvested 24 h after last media exchange, and L-lactate concentration was quantified by an enzyme-based assay. Data are presented as concentration (mM) measured by bioluminescent light release. $n = 5$ experiments. **B** L-lactate amount in supernatants of CM-treated macrophages. Cells were stimulated with CM 1:1 diluted in fresh growth media for 24 h. Total L-lactate in the supernatant was quantified by an enzyme-based assay. Data are presented as concentration (mM) measured by bioluminescent light release. $n = 5$ experiments. **C** L-lactate release by macrophages after CM stimulation. The amount of L-lactate released by macrophages was calculated by the total L-lactate concentration of macrophage supernatants minus the theoretical L-lactate concentration of CM 1:1 diluted in fresh growth medium. Data are presented as concentration (mM). $n = 5$ experiments. **D** Gene expression analysis of *Acod1*. Cells were stimulated with CM for 4 h and mRNA levels of *Acod1* were quantified by RT-qPCR. Data are presented as relative gene expression of gene of interest related to the reference gene *Hprt1*. $n = 5$ experiments. **E** Mitochondrial activity of macrophages. Cells were stimulated with CM for 24 h, and mitochondrial activity was measured by FACS analysis using a membrane potential-dependent fluorescent dye. Data are presented as median mitochondrial potential measured by fluorescence intensity. $n = 4$ experiments. **F** ATP production by macrophages. Cells were stimulated with CM for 24 h, and total ATP content was measured in cell lysates by enzyme-based assay (CTG). Data are presented as relative light units measured by bioluminescent light release. $n = 4$ experiments (mean of technical triplicates was included in statistics). For all, data are presented as mean + SD, and single values are shown as dots. *p*-values are calculated by ordinary one-way ANOVA with post hoc Bonferroni-corrected multiple comparison. Asterisk indicates significance against Medium, and number sign shows significance between respective planktonic and biofilm CM. $*p < 0.05$, $**p < 0.01$, $***p < 0.001$; $\#p < 0.05$, $\#\#p < 0.01$, $\#\#\#p < 0.001$. PC: positive control (1 µg/ml Pam3CSK4 + 100 nM CpG ODN).

concentrations of lactate added to high glucose medium and investigated the resulting macrophage cytokine response and metabolic activity as described previously. Compared to eukaryotes where L-lactate is the predominant form, SA is able to produce both enantiomers, respectively [35]. Thus, we included D-lactate in our investigations. Figure 4A shows that there were slight glucose concentration-dependent changes in the expression of *Tnfa* or *Il10*, which resulted in a statistically significant decrease in pro-inflammatory macrophage polarization (*Tnfα*/*Il10* ratio) in low glucose compared to a high glucose environment. The gene expression level of the glucose transporter *Slc2a1* was not affected by the amount of glucose in the medium (Fig. 4B). Different glucose concentrations also did not change basal or TLR induced mitochondrial activity (Fig. 4C). The increase in *Tnfa* mRNA levels observed upon TLR-2/-9 activation was further elevated by the addition of extracellular L-lactate. However, this was not accompanied by a change in *Il10* induction. In sum, this led to a concentration-dependent increase of pro-inflammatory macrophage polarization by extracellular L-lactate upon TLR-2/-9 activation (Fig. 4D). Interestingly, increasing extracellular L-lactate levels further enhanced the mitochondrial activity observed upon stimulation with PC (Fig. 4E). Adding D-lactate to the medium had no effect on the gene expression levels of *Tnfa* and led to an only slightly but not significantly ($p = 0.1989$ PC vs. PC + 20 mM) increase in induction of *Il10* mRNA levels not enough to change macrophage polarization (Fig. 4F). Eventually, the L-lactate present in the FCS of the cell culture medium has partially overshadowed the effects of D-lactate. This might equally explain, why the increasing D-lactate concentration led to an increase in mitochondrial activity upon TLR-2/-9 activation (Fig. 4G). We also investigated the effect of increasing extracellular acetate concentrations and found that gene expression levels of *Tnfa* only slightly ($p = 0.1046$ PC vs. PC + 20 mM) but those from *Il10* significantly increased at high acetate concentrations, which did not result in an overall change in pro-inflammatory macrophage polarization (Suppl. Figure 3).

In summary, our data indicate that low glucose or high lactate concentrations in the environment only have moderate effects on TLR-2/-9 mediated induction of *Tnfa* and *Il10* gene expression in macrophages. Although glucose and, partially, acetate can contribute to a more anti-inflammatory and L-lactate to a more pro-inflammatory macrophage immune response, the net effect remained comparatively small.

Low Glucose and High Lactate Concentrations Have No Effect on Macrophage IRF3 Mediated *Ifnb* Gene Expression Induced by SA Planktonic CM

We further investigated if different glucose and lactate concentrations affected the ability of macrophages to produce IFN-β in a SA planktonic environment. Therefore, we investigated IRF3 pathway activation and the subsequent induction of *Ifnb* gene expression to see if the low glucose and high lactate environment observed in SA biofilm CM could inhibit this pathway. We stimulated the cells with SA planktonic CM diluted in high or low glucose medium or added increasing concentrations of extracellular L- and D-lactate. Stimulation with SA biofilm CM was included for comparison. Figure 5A shows that glucose did not affect the increase in *Tnfa* and *Il10* mRNA levels observed for SA planktonic environment resulting in an unchanged macrophage polarization status. In addition, the induction of *Ifnb* gene expression and the IFN-β target gene *Isg15* remained unchanged by different extracellular glucose concentration (Fig. 5B). Consistently, activation of the NF-κB or IRF3 pathway by SA planktonic CM was independent of the extracellular glucose concentrations (Fig. 5C). Comparable results were seen for different L- (Figs. 5 D–G) and D- (Figs. 5 H–K) lactate concentrations. We could observe that the differences in induction of *Tnfa* and *Il10* gene expression and pro-inflammatory macrophage polarization between SA planktonic and SA biofilm CM were not triggered by the increased lactate concentrations characteristic for the biofilm environment (Figs. 5 D, H). Furthermore, *Ifnb* mRNA and p-IRF3 protein levels upon stimulation with SA planktonic CM were not affected by the addition of extracellular L- or D-lactate (Figs. 5 E, F, I, J). The cells responded to the higher extracellular L- or D-lactate concentrations with a slightly increased induction of *Il6* mRNA levels upon stimulation with SA planktonic CM when compared with conditions without lactate addition (Figs. 5 G, K). However, this increase did not reach the levels observed in the SA biofilm samples (Figs. 5 G, K).

Our data demonstrate that artificial low glucose and high lactate concentrations combined with the stimulation of macrophages with SA planktonic CM is not sufficient to induce a more anti-inflammatory macrophage immune response or to prevent IRF3 mediated *Ifnb* induction as seen in the respective biofilm environment.

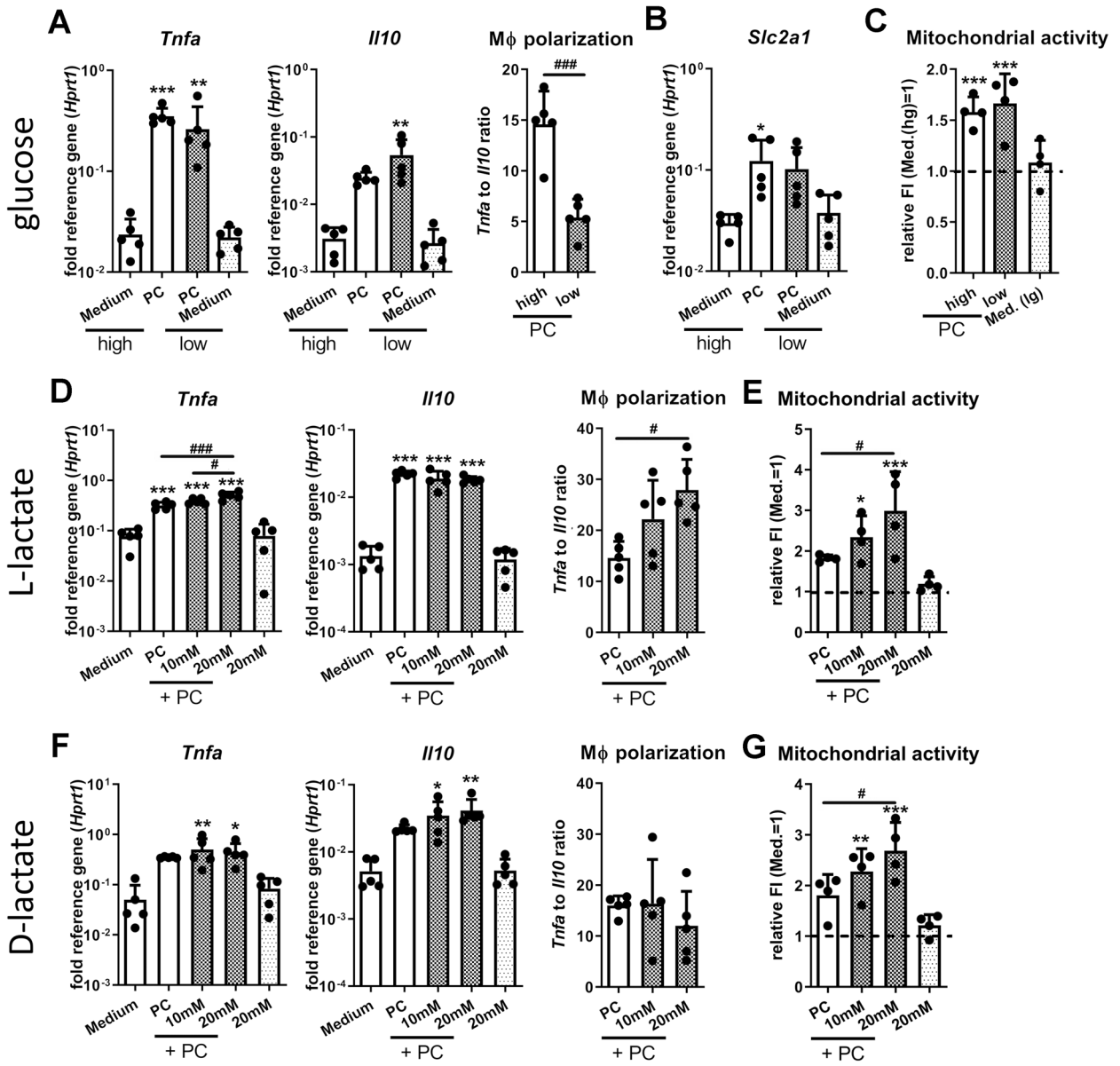

DISCUSSION

Biofilm formation is a major cause for the chronic progression of implant-related bone infections. The biofilm environment is discussed to shift the immune reaction towards a more tolerogenic response that supports bacterial persistence. Macrophages play an important role in the early defense against invading bacteria and their pro-inflammatory polarization is critical for effective bacterial clearance. In the present study, we wanted to investigate if the biofilm metabolite environment characterized by low glucose and high lactate levels is a main factor determining the intensity and direction of the macrophage immune response in planktonic versus biofilm infectious situations. In addition, we included two relevant bacteria strains, *Staphylococcus aureus* and *epidermidis*. SA is highly virulent, produces a panel of toxins, is able to survive intracellularly, and can form biofilms [12]. In contrast, the pathogenicity of SE mainly depends on biofilm formation [13]. To address

◀**Fig. 4** Effect of biofilm metabolite profile on macrophage TLR-2/-9 response. RAW 264.7 cells were stimulated with PC (positive control: 1 µg/ml Pam3CSK4 + 100 nM CpG ODN) for 20 h under low glucose or high lactate conditions, and cytokine response and mitochondrial activity were evaluated. **A**–**C** Effect of extracellular glucose concentration. Cells were stimulated by PC either in high (hg, 4.5 g/L) or low (lg, 1 g/L) glucose media. **A**, **B** Gene expression analysis of pro-inflammatory *Tnfa* and anti-inflammatory *Il10* (**A**) and glucose transporter *Slc2a1* (**B**). Ratio of *Tnfa* to *Il10* expression levels was used as indicator for macrophage polarization. Data are presented as relative gene expression of gene of interest related to the reference gene *Hprt1*. $n = 5$ experiments. **C** Mitochondrial activity was measured by FACS analysis using a membrane potential-dependent fluorescent dye. Data are presented as normalized fluorescence intensity with medium sample set as 1. $n = 4$ experiments. **D**, **E** Effect of extracellular L-lactate concentration. Cells were stimulated by PC in media supplemented with different L-lactate concentrations (10 and 20 mM). **D** Gene expression analysis of pro-inflammatory *Tnfa* and anti-inflammatory *Il10*. Ratio of *Tnfa* to *Il10* expression levels was used as indicator for macrophage polarization. Data are presented as relative gene expression of gene of interest related to the reference gene *Hprt1*. $n = 5$ experiments. **E** Mitochondrial activity was measured by FACS analysis using a membrane potential-dependent fluorescent dye. Data are presented as normalized fluorescence intensity with medium sample set as 1. $n = 4$ experiments. **F**, **G** Effect of extracellular D-lactate concentration. Cells were stimulated by PC in media supplemented with different D-lactate concentrations (10 and 20 mM). **G** Gene expression analysis of pro-inflammatory *Tnfa* and anti-inflammatory *Il10*. Ratio of *Tnfa* to *Il10* expression levels was used as indicator for macrophage polarization. Data are presented as relative gene expression of gene of interest related to the reference gene *Hprt1*. $n = 5$ experiments. **H** Mitochondrial activity was measured by FACS analysis using a membrane potential-dependent fluorescent dye. Data are presented as normalized fluorescence intensity with medium sample set as 1. $n = 4$ experiments. For all, data are presented as mean + SD, and single values are shown as dots. *p*-values are calculated by ordinary one-way ANOVA with post-hoc Bonferroni corrected multiple comparison. Asterisk indicates significance against Medium, and number sign shows significance between metabolite concentrations. $*p < 0.05$, $**p < 0.01$, $***p < 0.001$; $\#p < 0.05$, $\#\#p < 0.01$, $\#\#\#p < 0.001$.

this difference, we used the SE reference strain RP62A, which possesses a high *in vitro* biofilm formation capacity [32], and the SA strain UAMS-1, which originates from an osteomyelitis patient and shows only moderate biofilm formation on uncoated plastic surfaces [29, 31]. Independent of the different capacities in biofilm formation, the CM of both SA and SE shared similar characteristics with low glucose and high lactate levels in the biofilm CM, nicely representing glucose deprivation and lactate accumulation known for the local biofilm micromilieu [27, 28]. We cultivated RAW 264.7 macrophages in planktonic or biofilm CM generated from SA and SE cultures, respectively, and analyzed immune cell activation by measuring cell surface proteins, cytokine gene expression, metabolic activity, and underlying signal transduction events. We show that planktonic and biofilm environments both are able to elicit a predominantly pro-inflammatory immune response with increased glycolytic activity. However, this was less pronounced in biofilm CM, and the increased gene expression levels of the anti-inflammatory cytokine IL-10 support this finding. Our data further indicate that only planktonic bacteria are able to initiate an IRF7 mediated IFN-β response, which was not detected in the respective biofilm environment. Interestingly, only in SA planktonic CM, *Ifnb* induction was also associated with IRF3 pathway activation. This can be explained by the profuse arsenal of virulence factors expressed by planktonic SA which causes more severe immune reactions than SE. Mimicking the metabolite profile of the biofilm environment with low glucose or high lactate concentrations had no effect on macrophage cytokine induction after TLR-2/-9 activation or stimulation with SA planktonic CM. In summary, our data indicate that the biofilm environment indeed elicits a less strong immune activation and supports a more anti-inflammatory macrophage phenotype compared to the respective planktonic environment. This was confirmed for SA as well as for SE. Further, our data clearly show that mimicking the biofilm metabolite environment during stimulation with relevant TLR ligands or planktonic CM is insufficient to shift the macrophage immune response towards the biofilm situation. Thus, our results suggest that ultimately, differentially released pathogenicity factors by the bacteria either growing planktonic or in biofilm are the central mediators that shape the resulting immune response.

In line with previous data from SA biofilm infection models [21, 22], biofilm CM of SA and SE induced a less pronounced upregulation of TLR-2 surface localization compared to planktonic CM. Despite the reduced surface levels of TLR-2, MHCII, CD80 and CD86 in biofilm CM, planktonic as well as biofilm CM of both strains induced a comparable increase in NF-κB signaling that resulted in the expression of proportionate amounts of pro-inflammatory TNF-α. Equal or even increased TNF-α levels upon stimulation with supernatants generated from biofilm compared to planktonic SA cultures were also detected in human keratinocytes or fibroblasts [36, 37]. Our findings are in contrast to a similar study that found a suppression of pro-inflammatory macrophage activity by biofilm CM of SA which was mediated by KLF2 [38], a known negative regulator of NF-κB transcriptional activity [39]. The authors suggest that the observed increase in KLF2 expression might be caused by the secretion of

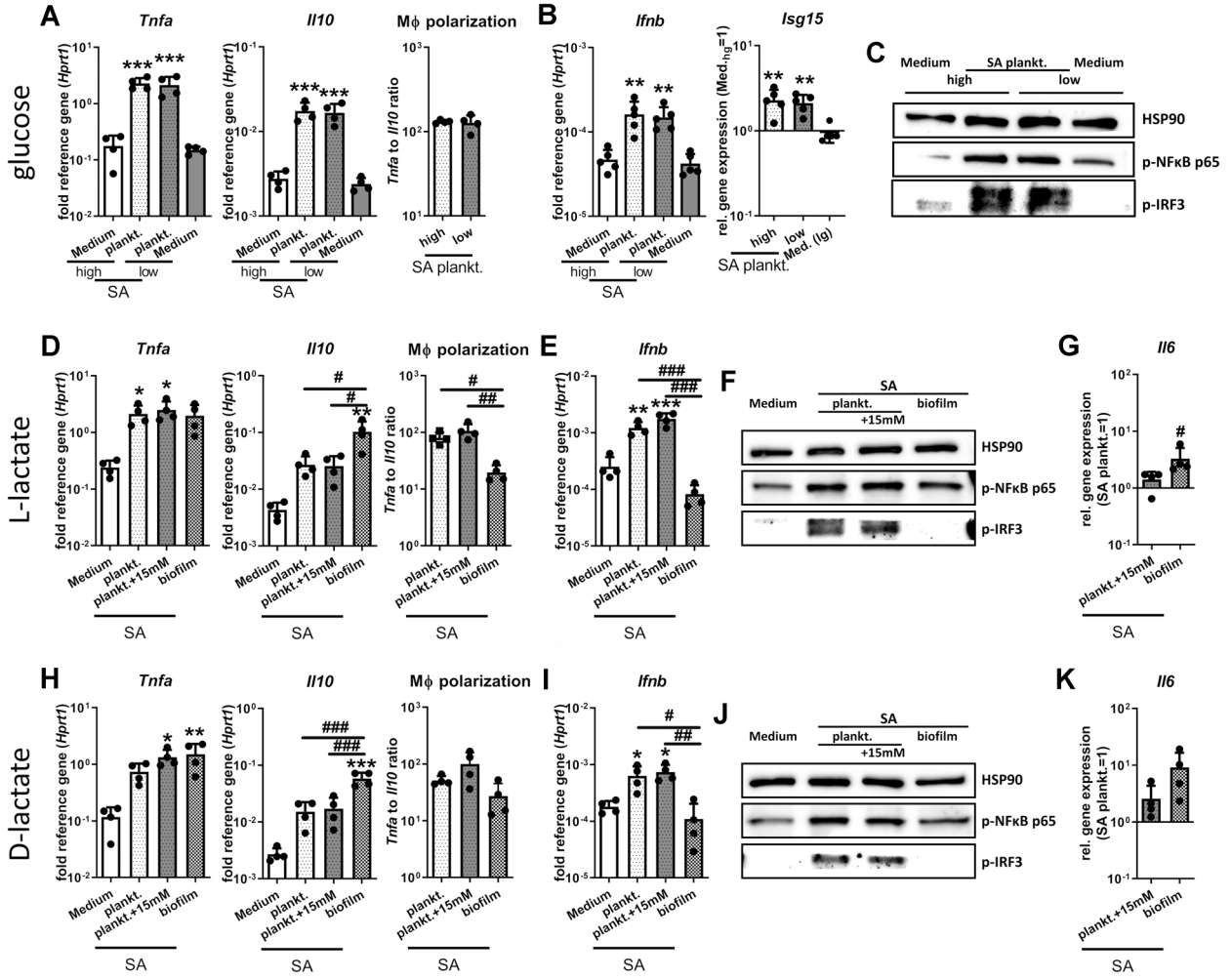

Fig. 5 Effect of biofilm metabolite profile on IRF3 mediated *Ifnb* induction by SA planktonic CM. RAW 264.7 cells were cultivated in SA plankt. 1:1 diluted in fresh growth media (DMEM high glucose + 10% FCS + 1% Pen/Strep) with different extracellular glucose or lactate concentrations and immune response was investigated. **A**–**C** Effect of extracellular glucose concentration. Cells were stimulated with SA plankt. CM 1:1 diluted either in high (hg, 4.5 g/L) or low (lg, 1 g/L) glucose media. **A**, **B** Gene expression analysis of pro-inflammatory *Tnfa* and anti-inflammatory *Il10* (**A**) and *Ifnb* (**B**) after 20 h of stimulation. The ratio of *Tnfa* to *Il10* expression levels was used as an indicator for macrophage polarization. Data are presented as relative gene expression of gene of interest related to the reference gene *Hprt1*. $n = 4$ or 5 experiments. **C** Activation of NF-κB and IRF3 signaling in macrophages. Cells were stimulated for 4 h, and the presence of phospho-NFκB p65 and phospho-IRF3 as activated forms of the transcription factors was visualized by western blot. HSP90 was used as loading control, $n = 3$ experiments. **D**–**G** Effect of extracellular L-lactate concentration. Cells were stimulated with SA plankt. CM 1:1 diluted in media ± 15 mM L-lactate or SA biofilm CM for comparison. **D**, **E** Gene expression analysis of pro-inflammatory *Tnfa* and anti-inflammatory *Il10* (**D**) and *Ifnb* (**E**) after 20 h of stimulation. The ratio of *Tnfa* to *Il10* expression levels was used as an indicator for macrophage polarization. Data are presented as relative gene expression of gene of interest related to the reference gene *Hprt1*. $n = 4$ experiments. **F** Activation of NF-κB and IRF3 signaling in macrophages. Cells were stimulated for 4 h, and the presence of phospho-NFκB p65 and phospho-IRF3 as activated forms of the transcription factors was visualized by western blot. HSP90 was used as loading control, $n = 3$ experiments. **G** Gene expression analysis of *Il6* after 20 h of stimulation. Data are presented as relative gene expression normalized on SA plankt. CM. $n = 4$ experiments. **H**–**K** Effect of extracellular D-lactate concentration. Cells were stimulated with SA plankt. CM 1:1 diluted in media ± 15 mM D-lactate. **G**, **H** Gene expression analysis of pro-inflammatory *Tnfa* and anti-inflammatory *Il10* (**G**) and *Ifnb* (**H**) after 20 h of stimulation. The ratio of *Tnfa* to *Il10* expression levels was used as an indicator for macrophage polarization. Data are presented as relative gene expression of gene of interest related to the reference gene *Hprt1*. $n = 4$ experiments. **J** Activation of NF-κB and IRF3 signaling in macrophages. Cells were stimulated for 4 h, and the presence of phospho-NFκB p65 and phospho-IRF3 as activated forms of the transcription factors was visualized by Western Blot. HSP90 was used as loading control, $n = 3$ experiments. **K** Gene expression analysis of *Il6* after 20 h of stimulation. Data are presented as relative gene expression normalized on SA plankt. CM. $n = 4$ experiments. For **A** and **B**; **D**, **E**, and **G**; **H**, **I**, and **K**, data are presented as mean + SD, and single values are shown as dots. *p*-values are calculated by ordinary one-way ANOVA with post hoc Bonferroni-corrected multiple comparison. Asterisk indicates significance against medium, and number sign shows significance between different treatments. $*p < 0.05$, $**p < 0.01$, $***p < 0.001$; $\#p < 0.05$, $\#\#p < 0.01$, $\#\#\#p < 0.001$.

class II exotoxins such as α-hemolysin into the environment. However, the UAMS-1 strain used in our study is negative for α-hemolysin due to a mutation of the *hla* gene [40], which might explain the different results. Further, the authors focused on *Il6* and *Il1b* gene expression and did not check for *Tnfa* gene expression which might be differentially regulated. Our data suggest that the initial release of pro-inflammatory cytokine TNF-α from macrophages might be less important in the inefficient immune response against biofilms than the subsequent initiation of a T-cell response through MHCII-mediated antigen presentation. As an impaired T-cell response is discussed as one of the reasons behind the chronicity of biofilm infections [7], effects of the biofilm environment on the macrophage/T-cell interaction should be investigated in more detail. Our experiments further demonstrated an induction of *Ifnb* gene expression in macrophages upon stimulation with planktonic CM of SA and SE. For SA infections, induction of an IFN-β response has been described previously [41]. Here, we showed that also SE is able to trigger IFN-β production. The direct comparison of *Ifnb* induction by planktonic and biofilm environments revealed that this specifically happens in the presence of a planktonic environment and is not triggered by the corresponding biofilm environment. Planktonic CM strongly induced TLR signaling that could have been one cause for the activation of the IRF7 pathway detected in these environments. For SA planktonic CM, an additional activation of IRF3 was observed, which can be a downstream target of cytosolic nucleic acid sensor pathways such as the cGAS-STING pathway [42]. A recent study showed that indeed STING-IRF3 signaling is involved in IFN-β induction upon infection of macrophages with live SA [43]. Another study showed that also SA biofilms can lead to a STING-dependent IFN-β induction in macrophages via the release of c-di-AMP due to bacterial lysis [44]. This is in contrast to our findings as we did not detect IRF3 activation and *Ifnb* induction in the biofilm environment which could be caused by the use of different SA strains, varying culturing conditions and experimental setups. In virus infections, IFN-β interferes with cellular proliferation and induces the production of ISGs that impairs viral replication [45]. It is becoming increasingly clearer that IFN-β has important but controversial functions in bacterial infections [46, 47]. The fact that *Ifnb* was dominantly expressed after incubation with planktonic bacteria that usually can be cleared through the immune system suggests that a focus should be set on investigating its role in the course of chronic implant-related bone infections. Metabolic analysis revealed that especially in the planktonic environments, the macrophage immune response is dominated by aerobic glycolysis. However, it could be observed that the cells started to enhance their mitochondrial activity upon stimulation with CM, which was most pronounced for CM derived from SE biofilm cultures. Increased OxPhos activity is associated with a more anti-inflammatory M2 macrophage polarization [26] and might play a role in chronic biofilm infections [28]. Our finding for SE biofilm CM is in line with a recent study, where a shift towards OxPhos activity was shown in monocytes over the time course of an orthopedic biofilm infection. Furthermore, the authors showed that inhibiting OxPhos *in vivo* by a nanoparticle-based delivery of oligomycin restored an effective pro-inflammatory monocyte immune response and reduced biofilm burden [48]. Extracellular lactate was found to be associated with an inhibitory effect on the pro-inflammatory immune response of macrophages [49–51]. In a recent study, the Kielian group compared the effects of biofilm-derived L- and D-lactate on the production of anti-inflammatory IL-10 using mutant SA strains deficient in L- and D-lactate production [35]. Their data suggest that biofilm-derived lactate is responsible for an increased IL-10 synthesis by myeloid-derived suppressor cells (MDSCs) and macrophages via inhibition of histone deacetylase 11 (HDAC11) and an unchecked *Il10* promotor activity. Although we detected high amounts of bacterial lactate only for biofilm CM, in our experimental setup, a strong *Il10* induction could be detected for both, planktonic and biofilm CM. In the biofilm CM, induction of *Il10* gene expression was higher than in the respective planktonic environment which might be due to its higher lactate concentration. As we did not detect bacterial lactate in planktonic CM, we suggest that the mechanisms behind *Il10* induction may differ between planktonic and biofilm environments. In addition, independently of bacterial-derived lactate concentrations, planktonic CM was able to induce *Il10* gene expression as a consequence of increased TLR signaling.

We further evaluated the effect of extracellular low glucose or high lactate levels on macrophage polarization upon TLR-2/-9 stimulation. Most studies have investigated the impact of extracellular lactate as a product of aerobic glycolysis triggered by LPS mediated TLR-4 signaling [52]. In these studies, high lactate concentrations were associated with a suppression of pro-inflammatory macrophage responses [49, 51], which was also seen for TLR-2 stimulation by Pam3Cys [50]. Conversely, we detected an increase of *Tnfa* mRNA levels with increasing extracellular L-lactate concentrations resulting in a

more pro-inflammatory macrophage polarization upon TLR-2/-9 activation. In comparison to our setup, the other studies used either higher lactate concentrations (up to 100 mM) or lactate pre-incubation before LPS treatment which might have led to different results. Furthermore, it is possible that the effects of lactate on the macrophage immune response vary between different TLR ligands. In addition, we observed that the addition of extracellular lactate dose-dependently enhanced mitochondrial activity after stimulation with TLR-2/-9 ligands, which after a longer time period of several days might lead to a metabolically induced switch towards a more anti-inflammatory response. Compared to lactate, the impact of extracellular glucose levels on a TLR-mediated immune response has been investigated to a lesser extent. High extracellular glucose levels were linked to LPS-induced inflammasome activation, pyroptosis and IL-1β production in macrophages [53, 54]. In our setting, we only observed minor effects of extracellular glucose levels on *Tnfa* and *Il10* gene expression levels after TLR-2/-9 stimulation. Nonetheless, the ratio between the two indicated that macrophage polarization shifted towards a less pro- and more anti-inflammatory response at low glucose levels. Mitochondrial activity, however, remained unaffected. In a paper investigating the effects of different glucose concentrations on LPS-mediated immune responses of macrophages from non-diabetic and diabetic mice [55], it was found that the effect of extracellular glucose concentrations on the LPS response was getting stronger over time. In line with our data, the authors detected only slight changes in cytokine release of healthy macrophages after 24 h, whereas higher glucose concentrations decreased TNF-α cytokine levels after 7 days of LPS stimulation. Furthermore, we investigated the effects of different extracellular glucose and lactate concentrations on the macrophage cytokine response upon stimulation with SA planktonic CM. Low glucose or the addition of lactate had no effect on the induction of *Tnfa* gene expression in response to SA planktonic CM nor increased *Il10* mRNA levels like in the SA biofilm CM. This clearly differed from our results observed for our bacterial CM which were shown by ^{1}H-NMR to contain low glucose and high lactate concentrations under biofilm conditions. Our data suggest that mimicking biofilm metabolite conditions in a planktonic environment by reducing glucose or adding lactate was not sufficient to shift the macrophage polarization towards the biofilm situation. Therefore, the difference in the macrophage activation profile is primarily dependent on further substances from the CM and not on the metabolite levels. Low glucose or high lactate levels also did not affect IRF3 activation and the subsequent induction of *Ifnb* gene expression upon stimulation with SA planktonic CM. This again indicates that the metabolite profile of the biofilm environment does not prevent the IRF3-mediated *Ifnb* induction. It rather seems that IFN-β production requires an additional bacterial stimulus that is present under planktonic conditions but missing in the biofilm environment. This is not unexpected, as the induction of bacterial genes associated with biofilm formation and metabolic adaption is often accompanied by a downregulation of virulence factors predominantly expressed in the planktonic lifestyle [56, 57]. Identifying these immunogenic, bacterial mediators might help to clarify the underlying mechanisms behind the impaired immune activation by the biofilm environment.

Our results were obtained in an indirect approach using a cell line; thus, the validation of the key findings in primary cells and in suitable co-culture systems is necessary. Nevertheless, our data clearly indicate that the presence or absence of bacterial factors differs between planktonic and biofilm environments and shapes the macrophage immune response rather than the different metabolite levels. The success of cancer immunotherapy suggests that immunomodulation might be an attractive novel treatment strategy for chronic biofilm-based infections associated with immune tolerance (reviewed in [7]). Our findings contribute to the identification of potential targets for an immunotherapeutic intervention with the aim to strengthen the immune response in chronic implant-related bone infections.

SUPPLEMENTARY INFORMATION

The online version contains supplementary material available at https://doi.org/10.1007/s10753-023-01824-3.

ACKNOWLEDGEMENTS

We would like to thank Katharina Draxel and Stella Cavicchioli for their help with the experiments. Furthermore, we thank Gabriele Sonnenmoser for the technical assistance.

AUTHOR CONTRIBUTION

ES was responsible for the study conception and design, acquisition, analysis, and interpretation of data and wrote the manuscript. TE and FVK participated in data acquisition, analysis, and interpretation. MSC was involved in data interpretation and critically revised the manuscript. KFK supervised the study, contributed to data interpretation, helped to draft the manuscript, and critically revised the manuscript. All authors read and approved the final manuscript.

FUNDING

Open Access funding enabled and organized by Projekt DEAL. Elisabeth Seebach was funded by the Physician Scientist Program of the Medical Faculty of Heidelberg University.

DATA AVAILABILITY

The raw data will be available on reasonable request.

Declarations

Conflict of Interest The authors declare no competing interests.

REFERENCES

1. Zimmerli, W., and P. Sendi. 2017. Orthopaedic biofilm infections. *APMIS* 125: 353–364. https://doi.org/10.1111/apm.12687.
2. Tande, A.J., and R. Patel. 2014. Prosthetic joint infection. *Clinical Microbiology Reviews* 27: 302–345. https://doi.org/10.1128/CMR.00111-13.
3. Otto, M. 2018. Staphylococcal Biofilms. *Microbiology Spectrum* 6.https://doi.org/10.1128/microbiolspec.GPP3-0023-2018.
4. Watters, C., D. Fleming, D. Bishop, and K.P. Rumbaugh. 2016. Host responses to biofilm. *Progress in Molecular Biology and Translational Science* 142: 193–239. https://doi.org/10.1016/bs.pmbts.2016.05.007.
5. Zimmerli, W., and P. Sendi. 2011. Pathogenesis of implant-associated infection: The role of the host. *Semin Immunopathol.* 33: 295–306. https://doi.org/10.1007/s00281-011-0275-7.
6. Arciola, C.R., D. Campoccia, and L. Montanaro. 2018. Implant infections: Adhesion, biofilm formation and immune evasion. *Nature Reviews Microbiology* 16: 397–409. https://doi.org/10.1038/s41579-018-0019-y.
7. Seebach, E., and K.F. Kubatzky. 2019. Chronic implant-related bone infections-can immune modulation be a therapeutic strategy? *Frontiers in Immunology* 10: 1724. https://doi.org/10.3389/fimmu.2019.01724.
8. Gries, C.M., and T. Kielian. 2017. Staphylococcal biofilms and immune polarization during prosthetic joint infection. *Journal of American Academy of Orthopaedic Surgeons* 25 (Suppl 1): S20–S24. https://doi.org/10.5435/JAAOS-D-16-00636.
9. Loffler, B., L. Tuchscherr, S. Niemann, and G. Peters. 2014. Staphylococcus aureus persistence in non-professional phagocytes. *International Journal of Medical Microbiology* 304: 170–176. https://doi.org/10.1016/j.ijmm.2013.11.011.
10. Krauss, J.L., P.M. Roper, A. Ballard, C.C. Shih, J.A.J. Fitzpatrick , J.E. Cassat, et al. 2019. Staphylococcus aureus infects osteoclasts and replicates intracellularly. *mBio* 10. https://doi.org/10.1128/mBio.02447-19.
11. Zoller, S.D., V. Hegde, Z.D.C. Burke, H.Y. Park, C.R. Ishmael, G.W. Blumstein, et al. 2020. Evading the host response: Staphylococcus "hiding" in cortical bone canalicular system causes increased bacterial burden. *Bone Res.* 8: 43. https://doi.org/10.1038/s41413-020-00118-w.
12. Muthukrishnan, G., E.A. Masters, J.L. Daiss, and E.M. Schwarz. 2019. Mechanisms of immune evasion and bone tissue colonization that make Staphylococcus aureus the primary pathogen in osteomyelitis. *Current Osteoporosis Reports* 17: 395–404. https://doi.org/10.1007/s11914-019-00548-4.
13. Le, K.Y., M.D. Park, and M. Otto. 2018. Immune evasion mechanisms of Staphylococcus epidermidis biofilm infection. *Frontiers in Microbiology* 9: 359. https://doi.org/10.3389/fmicb.2018.00359.
14. Foster, T.J. 2005. Immune evasion by staphylococci. *Nature Reviews Microbiology* 3: 948–958. https://doi.org/10.1038/nrmicro1289.
15. Masters, E.A., R.P. Trombetta, K.L. de Mesy Bentley, B.F. Boyce, A.L. Gill, S.R Gill, et al. 2019. Evolving concepts in bone infection: redefining "biofilm", "acute vs. chronic osteomyelitis", "the immune proteome" and "local antibiotic therapy". *Bone Res* 7: 20. https://doi.org/10.1038/s41413-019-0061-z.
16. Zimmerli, W., A. Trampuz, and P.E. Ochsner. 2004. Prosthetic-joint infections. *New England Journal of Medicine* 351: 1645–1654. https://doi.org/10.1056/NEJMra040181.
17. Kawai, T., and S. Akira. 2010. The role of pattern-recognition receptors in innate immunity: Update on Toll-like receptors. *Nature Immunology* 11: 373–384. https://doi.org/10.1038/ni.1863.
18. Kufer, T.A., and P.J. Sansonetti. 2007. Sensing of bacteria: NOD a lonely job. *Current Opinion in Microbiology* 10: 62–69. https://doi.org/10.1016/j.mib.2006.11.003.
19. Marinho, F.V., S. Benmerzoug, S.C. Oliveira, B. Ryffel, and V.F.J. Quesniaux. 2017. The emerging roles of STING in bacterial infections. *Trends in Microbiology* 25: 906–918. https://doi.org/10.1016/j.tim.2017.05.008.
20. Pietrocola, G., C.R. Arciola, S. Rindi, A. Di Poto, A. Missineo, L. Montanaro, et al. 2011. Toll-like receptors (TLRs) in innate immune defense against Staphylococcus aureus. *International Journal of Artificial Organs* 34: 799–810. https://doi.org/10.5301/ijao.5000030.
21. Thurlow, L.R., M.L. Hanke, T. Fritz, A. Angle, A. Aldrich, S.H. Williams, et al. 2011. Staphylococcus aureus biofilms prevent macrophage phagocytosis and attenuate inflammation in vivo. *The Journal of Immunology* 186: 6585–6596. https://doi.org/10.4049/jimmunol.1002794.
22. Bernthal, N.M., J.R. Pribaz, A.I. Stavrakis, F. Billi, J.S. Cho, R.I. Ramos, et al. 2011. Protective role of IL-1beta against post-arthroplasty Staphylococcus aureus infection. *Journal of Orthopaedic Research* 29: 1621–1626. https://doi.org/10.1002/jor.21414.
23. Murray, P.J., and T.A. Wynn. 2011. Protective and pathogenic functions of macrophage subsets. *Nature Reviews Immunology* 11: 723–737. https://doi.org/10.1038/nri3073.
24. Sica, A., and A. Mantovani. 2012. Macrophage plasticity and polarization: In vivo veritas. *The Journal of Clinical Investigation* 122: 787–795. https://doi.org/10.1172/JCI59643.

25. Benoit, M., B. Desnues, and J.L. Mege. 2008. Macrophage polarization in bacterial infections. *The Journal of Immunology* 181: 3733–3739. https://doi.org/10.4049/jimmunol.181.6.3733.
26. Kelly, B., and L.A. O'Neill. 2015. Metabolic reprogramming in macrophages and dendritic cells in innate immunity. *Cell Research* 25: 771–784. https://doi.org/10.1038/cr.2015.68.
27. Zhu, Y., E.C. Weiss, M. Otto, P.D. Fey, M.S. Smeltzer, and G.A. Somerville. 2007. Staphylococcus aureus biofilm metabolism and the influence of arginine on polysaccharide intercellular adhesin synthesis, biofilm formation, and pathogenesis. *Infection and Immunity* 75: 4219–4226. https://doi.org/10.1128/IAI.00509-07.
28. Yamada, K.J., and T. Kielian. 2019. Biofilm-leukocyte cross-talk: Impact on immune polarization and immunometabolism. *Journal of Innate Immunity* 11: 280–288. https://doi.org/10.1159/000492680.
29. Gillaspy, A.F., S.G. Hickmon, R.A. Skinner, J.R. Thomas, C.L. Nelson, and M.S. Smeltzer. 1995. Role of the accessory gene regulator (agr) in pathogenesis of staphylococcal osteomyelitis. *Infection and Immunity* 63: 3373–3380. https://doi.org/10.1128/IAI.63.9.3373-3380.1995.
30. Raschke, W.C., S. Baird, P. Ralph, and I. Nakoinz. 1978. Functional macrophage cell lines transformed by Abelson leukemia virus. *Cell* 15: 261–267. https://doi.org/10.1016/0092-8674(78)90101-0.
31. Beenken, K.E., J.S. Blevins, and M.S. Smeltzer. 2003. Mutation of sarA in Staphylococcus aureus limits biofilm formation. *Infection and Immunity* 71: 4206–4211. https://doi.org/10.1128/iai.71.7.4206-4211.2003.
32. Christensen, G.D., W.A. Simpson, J.J. Younger, L.M. Baddour, F.F. Barrett, D.M. Melton, et al. 1985. Adherence of coagulase-negative staphylococci to plastic tissue culture plates: A quantitative model for the adherence of staphylococci to medical devices. *Journal of Clinical Microbiology* 22: 996–1006. https://doi.org/10.1128/JCM.22.6.996-1006.1985.
33. Lampropoulou, V., A. Sergushichev, M. Bambouskova, S. Nair, E.E. Vincent, E. Loginicheva, et al. 2016. Itaconate links inhibition of succinate dehydrogenase with macrophage metabolic remodeling and regulation of inflammation. *Cell Metabolism* 24: 158–166. https://doi.org/10.1016/j.cmet.2016.06.004.
34. O'Neill, L.A.J., and M.N. Artyomov. 2019. Itaconate: The poster child of metabolic reprogramming in macrophage function. *Nature Reviews Immunology* 19: 273–281. https://doi.org/10.1038/s41577-019-0128-5.
35. Heim, C.E., M.E. Bosch, K.J. Yamada, A.L. Aldrich, S.S. Chaudhari, D. Klinkebiel, et al. 2020. Lactate production by Staphylococcus aureus biofilm inhibits HDAC11 to reprogramme the host immune response during persistent infection. *Nature Microbiology* 5: 1271–1284. https://doi.org/10.1038/s41564-020-0756-3.
36. Secor, P.R., G.A. James, P. Fleckman, J.E. Olerud, K. McInnerney, and P.S. Stewart. 2011. Staphylococcus aureus biofilm and planktonic cultures differentially impact gene expression, mapk phosphorylation, and cytokine production in human keratinocytes. *BMC Microbiology* 11: 143. https://doi.org/10.1186/1471-2180-11-143.
37. Kirker, K.R., G.A. James, P. Fleckman, J.E. Olerud, and P.S. Stewart. 2012. Differential effects of planktonic and biofilm MRSA on human fibroblasts. *Wound Repair Regen.* 20: 253–261. https://doi.org/10.1111/j.1524-475X.2012.00769.x.
38. Alboslemy, T., B. Yu, T. Rogers, and M.H. Kim. 2019. Staphylococcus aureus biofilm-conditioned medium impairs macrophage-mediated antibiofilm immune response by upregulating KLF2 expression. *Infection and Immunity* 87. https://doi.org/10.1128/IAI.00643-18.
39. Das, H., A. Kumar, Z. Lin, W.D. Patino, P.M. Hwang, M.W. Feinberg, et al. 2006. Kruppel-like factor 2 (KLF2) regulates proinflammatory activation of monocytes. *Proc Natl Acad Sci U S A.* 103: 6653–6658. https://doi.org/10.1073/pnas.0508235103.
40. Herbert, S., A.K. Ziebandt, K. Ohlsen, T. Schafer, M. Hecker, D. Albrecht, et al. 2010. Repair of global regulators in Staphylococcus aureus 8325 and comparative analysis with other clinical isolates. *Infection and Immunity* 78: 2877–2889. https://doi.org/10.1128/IAI.00088-10.
41. Scumpia, P.O., G.A. Botten, J.S. Norman, K.M. Kelly-Scumpia, R. Spreafico, A.R. Ruccia, et al. 2017. Opposing roles of Toll-like receptor and cytosolic DNA-STING signaling pathways for Staphylococcus aureus cutaneous host defense. *PLoS Pathogens* 13: e1006496. https://doi.org/10.1371/journal.ppat.1006496.
42. Sun, L., J. Wu, F. Du, X. Chen, and Z.J. Chen. 2013. Cyclic GMP-AMP synthase is a cytosolic DNA sensor that activates the type I interferon pathway. *Science* 339: 786–791. https://doi.org/10.1126/science.1232458.
43. Zhou, Y., S. Zhao, X. Gao, S. Jiang, J. Ma, R. Wang, et al. 2021. Staphylococcus aureus induces IFN-beta production via a CARMA3-independent mechanism. *Pathogens* 10.https://doi.org/10.3390/pathogens10030300.
44. Gries, C.M., E.L. Bruger, D.E. Moormeier, T.D. Scherr, C.M. Waters, and T. Kielian. 2016. Cyclic di-AMP released from Staphylococcus aureus biofilm induces a macrophage type I interferon response. *Infection and Immunity* 84: 3564–3574. https://doi.org/10.1128/IAI.00447-16.
45. Katze, M.G., Y. He, and M. Gale Jr. 2002. Viruses and interferon: A fight for supremacy. *Nature Reviews Immunology* 2: 675–687. https://doi.org/10.1038/nri888.
46. Boxx, G.M., and G. Cheng. 2016. The roles of type I interferon in bacterial infection. *Cell Host & Microbe* 19: 760–769. https://doi.org/10.1016/j.chom.2016.05.016.
47. Kovarik, P., V. Castiglia, M. Ivin, and F. Ebner. 2016. Type I interferons in bacterial infections: A balancing act. *Frontiers in Immunology* 7: 652. https://doi.org/10.3389/fimmu.2016.00652.
48. Yamada, K.J., C.E. Heim, X. Xi, K.S. Attri, D. Wang, W. Zhang, et al. 2020. Monocyte metabolic reprogramming promotes pro-inflammatory activity and Staphylococcus aureus biofilm clearance. *PLoS Pathogens* 16: e1008354. https://doi.org/10.1371/journal.ppat.1008354.
49. Yang, K., J. Xu, M. Fan, F. Tu, X. Wang, T. Ha, et al. 2020. Lactate suppresses macrophage pro-inflammatory response to LPS stimulation by inhibition of YAP and NF-kappaB activation via GPR81-mediated signaling. *Front Immunology* 11: 587913. https://doi.org/10.3389/fimmu.2020.587913.
50. Ratter, J.M., H.M.M. Rooijackers, G.J. Hooiveld, A.G.M. Hijmans, B.E. de Galan, C.J. Tack, et al. 2018. In vitro and in vivo effects of lactate on metabolism and cytokine production of human primary PBMCs and monocytes. *Frontiers in Immunology* 9: 2564. https://doi.org/10.3389/fimmu.2018.02564.
51. Errea, A., D. Cayet, P. Marchetti, C. Tang, J. Kluza, S. Offermanns, et al. 2016. Lactate inhibits the pro-inflammatory response and metabolic reprogramming in murine macrophages in a GPR81-independent manner. *PLoS One* 11: e0163694.https://doi.org/10.1371/journal.pone.0163694.
52. Manoharan, I., P.D. Prasad, M. Thangaraju, and S. Manicassamy. 2021. Lactate-dependent regulation of immune responses by dendritic cells and macrophages. *Front Immunol*ogy 12: 691134.https://doi.org/10.3389/fimmu.2021.691134.
53. Aki, T., T. Funakoshi, K. Noritake, K. Unuma, and K. Uemura. 2020. Extracellular glucose is crucially involved in the fate decision of LPS-stimulated RAW264.7 murine macrophage cells. *Scientific Reports* 10: 10581. https://doi.org/10.1038/s41598-020-67396-6.
54. Pavlou, S., J. Lindsay, R. Ingram, H. Xu, and M. Chen. 2018. Sustained high glucose exposure sensitizes macrophage responses

to cytokine stimuli but reduces their phagocytic activity. *BMC Immunology* 19: 24. https://doi.org/10.1186/s12865-018-0261-0.

55. Ayala, T.S., F.H.G. Tessaro, G.P. Jannuzzi, L.M. Bella, K.S. Ferreira, and J.O. Martins. 2019. High glucose environments interfere with bone marrow-derived macrophage inflammatory mediator release, the TLR4 pathway and glucose metabolism. *Science and Reports* 9: 11447. https://doi.org/10.1038/s41598-019-47836-8.
56. Resch, A., R. Rosenstein, C. Nerz, and F. Gotz. 2005. Differential gene expression profiling of Staphylococcus aureus cultivated under biofilm and planktonic conditions. *Applied and Environment Microbiology* 71: 2663–2676. https://doi.org/10.1128/AEM.71.5.2663-2676.2005.
57. Resch, A., S. Leicht, M. Saric, L. Pasztor, A. Jakob, F. Gotz, et al. 2006. Comparative proteome analysis of Staphylococcus aureus biofilm and planktonic cells and correlation with transcriptome profiling. *Proteomics* 6: 1867–1877. https://doi.org/10.1002/pmic.200500531.